

Planck Mean Absorption Coefficients of H₂O, CO₂, CO and NO for radiation numerical modeling in combusting flows

Maciej Chmielewski*, Marian Gieras

*Warsaw University of Technology, Institute of Heat Engineering
Nowowiejska Street 21/25, 00-665 Warsaw*

Abstract

The Weighted-Sum-of-Gray-Gases Model (WSGGM), based on temperature dependent weighting factors, is an efficient method of determining the absorption coefficients in numerical modeling of combusting flows. Weighting factors are obtained by polynomial fitting of experimental data for only two reagents (H₂O and CO₂) to the analytical equation for emissivity. In this article the use of Planck Mean Absorption Coefficients (PMAC) for H₂O, CO₂, CO and NO in combustion numerical modeling is proposed. The aim of the PMAC approach is to improve the initial solution of temperature and species mass fraction profiles in numerical modeling of non-premixed methane combustion. The proposed model is verified against the results of turbulent, non-premixed methane combustion experimental data. The implemented PMAC model represents the flue gas composition and temperature more accurately than the WSGGM.

Keywords: radiation modeling, combustion, Planck mean absorption coefficient, weighted sum of gray gases

1. Introduction

It has been proven [1–7] that, mainly due to high temperatures, radiative heat transfer has a significant impact on combustion parameters. Therefore accurate prediction of temperatures and hence on emissions in combustion numerical modeling is strongly dependent on exact radiation modeling. The problem is particularly challenging in combustion modeling in turbine engines [2, 4, 6]. In commercial CFD codes the Weighted-Sum-of-Gray-Gases Model based on polynomial regression of experimental data for an H₂O and CO₂ mixture is implemented, as these are the main but not the only radiating species for hydrocarbon flames.

The aim of this article is to calculate the absorption coefficient as a weighted sum of Planck Mean Absorption Coefficients (PMAC) of particular combustion reagents based on their partial pressures. Some effort has been

made to describe the mean absorption coefficient by the weighted average of gray gases absorption coefficients based on partial pressures. In [8], absorption coefficients were calculated using RADCAL software [9] for some of the combustion reagents: H₂O, CO₂, CH₄ and CO. It was observed [10] that the inclusion of CH₄, and CO in OPPDIF (opposed-flow diffusion flame) calculations (modified to include radiation) of methane/air flames dropped the peak temperature by 5K. On the rich side of the same flames the maximum observed effect of adding CH₄ and CO radiation was an 8K reduction in temperature (from 1280K to 1272K for a particular location) compared with the the model including only an H₂O and CO₂ mixture.

The approach presented in this article assumes use of the Planck Mean Absorption Coefficient obtained from the high-resolution HITEMP database [11] for H₂O, CO₂, CO and NO. These four species have been selected because of their vital role in combustion modeling. Nowadays studies of emissions of carbon and nitrogen monoxides, mainly due to requirements for cleaner combustion systems, call for advanced modeling of the above species concentrations and hence their participation in the radia-

*Corresponding author

Email addresses: chmielfam@wp.pl (Maciej Chmielewski*), marian.gieras@itc.pw.edu.pl (Marian Gieras)

tive heat transfer. The proposed model aims to enable more accurate (compared to the currently used WSGGM model) initial solutions of combusting flow fields.

Partial pressures of particular gases are used as average wide-band absorption coefficient weights. The approach described in this article is planned for use in the numerical simulation of combustion inside a small turbine engine combustion chamber. The proposed Planck Mean Absorption Coefficient Model is implemented into the ANSYS FLUENT commercial CFD code. Numerical results are verified through comparison with experimental data. The test case is a turbulent non-premixed methane combustion with swirling air. Experimental data are obtained from research conducted at the University of Sydney [12–16].

2. Radiation numerical modeling

Currently, one of the most commonly used radiation models for combustion modeling is the Discrete Ordinates (DO) model. The DO model became popular in combustion modeling mainly due to the moderate computational cost and modest memory requirements. The DO model transforms the radiation transfer equation (RTE) into a transport equation for radiation intensity in n -dimensional coordinates. The model considers RTE in the direction \vec{s} as field equation [17]:

$$\Delta(I(\vec{r}, \vec{s})\vec{s}) + (\kappa + \sigma_s)I(\vec{r}, \vec{s}) = \kappa n^2 \frac{\sigma T^4}{\pi} + \frac{\sigma_s}{4\pi} \int_0^{4\pi} I(\vec{r}, \vec{s}') \Phi(\vec{s}, \vec{s}') d\Omega' \quad (1)$$

where: \vec{r} - positional vector, \vec{s} - directional vector, \vec{s}' - scattering direction vector, s - path length, κ - absorption coefficient, n - refractive index, σ_s - scattering coefficient, σ - Stefan – Boltzmann constant, I - radiation intensity, Φ - phase function, Ω' - solid angle.

The DO model requires the absorption coefficient as coefficient as an input. This can be noticed from (1). In ANSYS Fluent, the Weighted-Sum-of-Gray-Gases-Model (WSGGM) is implemented. This is a default choice for modeling radiation in combusting flows. It has been developed as a compromise between the oversimplified gray gas model and a complete model which takes into account particular absorption bands.

The WSGGM approach assumes that total emissivity over distance s can be described by:

$$\epsilon = \sum_{i=0}^n a_{\epsilon,i}(T)(1 - e^{-\kappa_i p s}) \quad (2)$$

where: $a_{\epsilon,i}$ - emissivity weighting factor for i^{th} gas, κ_i - absorption coefficient of i^{th} gas, p - sum of partial pressures of all absorbing gases, s - path length.

For the $i = 0$ absorption coefficient value is set to zero ($\kappa_0 = 0$), simultaneously the weighting factor for $i = 0$ is set as complement to unity:

$$a_{\epsilon,0} = 1 - \sum_{i=1}^n a_{\epsilon,i} \quad (3)$$

In the case of the other gases, the weighting factor is temperature dependent and is approximated by:

$$a_{\epsilon,i} = 1 - \sum_{j=1}^N b_{\epsilon,i,j} T^{j-1} \quad (4)$$

where: $b_{\epsilon,i,j}$ are a gas temperature polynomial coefficients, which like κ_i are obtained by fitting (2) to experimental data. ANSYS Fluent finally calculates the absorption coefficient as:

$$\kappa = \frac{\ln(1 - \epsilon)}{s}: \text{ for } s > 10^{-4} \text{ m} \quad (5)$$

$$\kappa = \sum_{j=1}^N a_{\epsilon,i} \kappa_i p: \text{ for } s \leq 10^{-4} \text{ m} \quad (6)$$

Traditional WSGGM relies on the use of two separate formulations depending on the path length. As was mentioned, ANSYS Fluent uses experimental data from [18] and [19] where polynomial functions have been fitted to experimental data only for particular CO₂ and H₂O mixtures.

3. Proposed approach

The proposed approach assumes that each computational cell is occupied by a gray gas consisting of a mixture of combustion reagents. Each combustion reagent occupies its own portion of the cell. The ratio of radiation path lengths of each species to radiation path length of the whole cell is equal to the partial volume of each species to the total volume of the cell ratio. Based on Amagat's law of additive volume for ideal gas inside the computational cell:

$$\frac{s_i}{s_{tot}} = \frac{V_i}{V_{tot}} = \frac{n_i}{n_{tot}} = \frac{p_i}{p_{tot}} \quad (7)$$

where: s_i - path length of the i^{th} gas mixture component, s_{tot} - total path length of gas mixture, V_i - partial volume of the i^{th} gas mixture component, V_{tot} - total volume of gas mixture, p_i - partial pressure of the i^{th} gas mixture component, p_{tot} - total pressure of gas mixture, n_i - amount of

moles of the i^{th} gas mixture component, n_{tot} - total amount of moles in gas mixture.

For such mixture, the radiative heat flux loss per unit volume can be calculate as:

$$q_{loss} = \sum_{i=1}^N p_i \kappa_i \sigma (T^4 - T_b^4) \quad (8)$$

where: κ_i - Planck mean absorption coefficient for i^{th} species (m Pa^{-1}), T - cell temperature, T_b - background temperature. Putting (7) to (8):

$$q_{loss} = \sum_{i=1}^N \frac{x_i}{x_{tot}} p_{tot} \kappa_i \sigma (T^4 - T_b^4) \quad (9)$$

Marking mixture weighted absorption coefficient as κ_{mix} (m^{-1}), based on (9) one can calculate:

$$\kappa_{mix} = \sum_{i=1}^N \frac{n_i}{n_{tot}} p_{tot} \kappa_i = p_{tot} \sum_{i=1}^N x_i \kappa_i \quad (10)$$

where: x_i - molar fraction of the i^{th} gas mixture component.

Planck mean absorption coefficients for individual gas species are calculated based on data from HITEMP 2010 high-resolution database [11] using approach developed in [20]:

$$\kappa_i = \frac{\pi}{\sigma T^4} \int_0^{\infty} I_{b\eta} \sum_j \kappa_{\eta j} d\eta = \sum_j \left(\frac{\pi I_{b\eta_0}}{\sigma T^4} \right) S_j \quad (11)$$

where: η - wavenumber (m^{-1}), S_j - j^{th} line integrated absorption coefficient, $I_{b\eta}$ - blackbody radiative intensity for given wave number ($I_{b\eta_0}$ is evaluated at the center of each spectral line), $\kappa_{\eta j}$ - absorption coefficient for given wavenumber.

Individual functions were fitted to the experimental data using Curve Fitting Tool (cftool) from Matlab. A number of different fit types were tested: Exponential, Fourier, Gaussian, Polynomial, Power and Sum of Sin function. Best fit was judged based on the sum of the squared errors of prediction - SSE (12) and the coefficient of determination - R^2 (13):

$$SSE = \sum_{j=1}^n (\kappa_j - f(T_j))^2 \quad (12)$$

$$R^2 = 1 - \frac{\sum_j (\kappa_j - f(T_j))^2}{\sum_j (\kappa_j - \bar{\kappa})^2} \quad (13)$$

where: κ_j - j^{th} value of absorption coefficient, T_j - j^{th} value of the temperature, $f(T_j)$ - predicted value of absorption coefficient, $\bar{\kappa}$ - mean absorption coefficient:

$$\bar{\kappa} = \frac{1}{n} \sum_{j=1}^n \kappa_j \quad (14)$$

Table 1 contains the SSE and R^2 for each of the considered fit functions. Shaded cells indicate the chosen fit function. Fitting function coefficients are presented in Table 2 for individual species. Where fit functions are described by following functions [21]:

Exponential:

- one-term:

$$\kappa(T) = \alpha e^{\beta T} \quad (15)$$

- two-term:

$$\kappa(T) = \alpha e^{\beta T} + \gamma e^{\delta T} \quad (16)$$

Fourier n^{th} degree:

$$\kappa(T) = \sum_{i=0}^n [\alpha_i \cos(i\omega T) + \beta_i \sin(i\omega T)] \quad (17)$$

Gaussian n -th degree:

$$\kappa(T) = \sum_{i=0}^n \alpha_i e^{-\left(\frac{T-\beta_i}{\gamma_i}\right)^2} \quad (18)$$

Polynomial n -th degree:

$$\kappa(T) = \sum_{i=0}^n \alpha_i T^{n+1-i} \quad (19)$$

Power:

- one-term:

$$\kappa(T) = \alpha T^{\beta} \quad (20)$$

- two-term:

$$\kappa(T) = \alpha + \beta T^{\gamma} \quad (21)$$

Sum of Sines:

$$\kappa(T) = \sum_{i=0}^n \alpha_i \sin(\beta_i T + \gamma_i) \quad (22)$$

The obtained Planck mean absorption coefficients are presented in the form of points in Figure 1 and Figure 2 for the temperature range 300-2500K. Figure 1 additionally shows PMAC curve fits for an H_2O and CO_2 developed in [22] with the use of RADCAL software. In Figure 2, fit

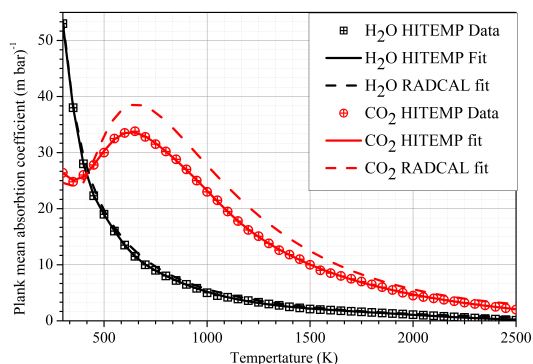


Figure 1: Planck mean absorption coefficient fitting functions against experimental data for H_2O and CO_2

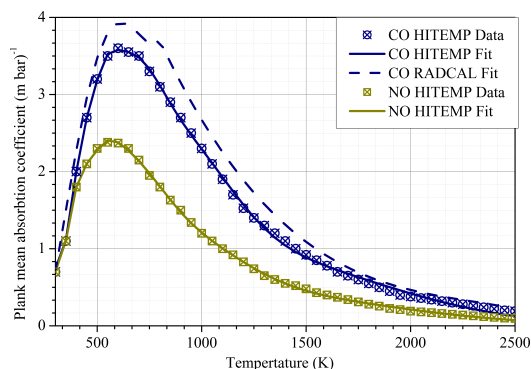


Figure 2: Planck mean absorption coefficient fitting functions against experimental data for CO and NO

of Planck mean absorption coefficients for a CO obtained from RADCAL is shown. It can be noticed that PMAC calculated using HITEMP for an H_2O are very close to coefficients from RADCAL (maximum difference of 9% noticed for 750K). Despite similar profiles of PMAC calculated using HITEMP and RADCAL, there are significant differences for a CO_2 and CO (21% for 1500K and 20% for 1200K respectively). A mismatch of a CO RADCAL fit curve at 750K proposed in [22] is also worth noticing. This mismatch is a result of two different fit functions for the specific temperature ranges.

Equation (10) is valid for all combustion species. Since four combustion species are considered, direct use of the same equation assigns an absorption coefficient of zero for the other ingredients. In reality the other species have a nonzero absorption coefficient. Combustion compounds other than H_2O , CO_2 , CO and NO (also CH_4 , but data for methane is unavailable in HITEMP 2010) have low concentrations in most combustion systems. Based on the above, the assumption that the absorption coefficients of the other species are equal to zero is an appropriate approximation of reality. Therefore, the absorption coefficient is calculated by (10). The proposed approach was successfully programmed in C language and implemented into the commercial ANSYS FLUENT code.

4. Results and discussion

Comparison and evaluation of the proposed PMAC Model were carried out on the basis of the Swirling Turbulent Non-premixed Flames of Methane experiment Comparison and evaluation of the proposed PMAC Model was carried out on the basis of Swirling Turbulent Non-premixed Flames of Methane experiment [12–16] which is the official verification test case for ANSYS Fluid Dynamics software [23]. In the experiment, methane and swirling jet

Table 2: Fitting function coefficients.

	H_2O	CO_2	CO	NO
α_1	63.87	34.57	0.9245	0.7796
β_1	149.5	45.32	503.1	487
γ_1	174.3	838.4	106.3	146.6
α_2	2.629	1.22	1.51	1.02
β_2	493.6	930.2	630.9	630.2
γ_2	111.1	184.9	200.3	231.3
α_3	222.9	-22.32	0.4082	0.3197
β_3	-2110	323.9	418	411.3
γ_3	1592	217.9	44.18	45.63
α_4	0.991	17.14	1.571	0.793
β_4	1700	92.98	845.4	834.5
γ_4	619.2	1657	371.8	425.3
α_5	—	—	0.94	0.4517
β_5	—	—	1139	1091
γ_5	—	—	959.2	1044

air are supplied from separate inlets of the burner. Non-swirling co-flow of air is present around the swirling air jet. Geometry and boundary conditions for numerical simulations are the same as for the experiment. The methane inlet has a diameter of 3.6 mm, while the swirling air inlet has an inner diameter of 50 mm and an outer diameter of 60 mm. The area of co-flow was limited to a cylinder with a diameter of 310 mm and length of 950 mm. Since a 2D axisymmetric swirl numerical calculations are performed, the computational domain is modeled as half of a cylinder slice (Fig. 3).

The parameters set in numerical calculations were the following: methane inlet velocity: 32.7 m/s, swirling air axial velocity: 38.2 m/s, swirl velocity: 19.1 m/s. Co-flowing air velocity was 20 m/s. The non-premixed equilibrium model with non-adiabatic energy treatment and probability density function was used. Turbulence was

Table 1: Sum of squared errors of prediction and coefficients of determination for individual fitting functions to experimental data.

Species	Indicator	Exponential			Fourier			Gaussian			Polynomial			Power			Sum of Sin fun							
		1-term	2-term	4-deg	4-deg	5-deg	5-deg	4-deg	4-deg	5-deg	5-deg	4-deg	4-deg	5-deg	1-term	5deg	1-term	2-term	4-deg	5-deg				
H ₂ O	<i>SSE</i>	157.3	3.324	4.115	0.9582	0.1877	0.4398	162.8	67.15	8.222	8.005	85.35	42.66	0.968	0.9993	0.9989	1.0000	0.9999	0.9669	0.9864	0.9983	0.9984	0.9827	0.9913
	<i>R</i> ²	0.968	0.9993	0.9989	0.9998	1.0000	0.9999	0.9669	0.9864	0.9983	0.9984	0.9827	0.9913	0.9999	0.9999	0.9999	0.9999	0.9999	0.9999	0.9999	0.9999	0.9999	0.9999	0.9999
CO ₂	<i>SSE</i>	836.5	74.2	3.646	1.193	0.5409	0.7961	55.34	46.88	1872	559.9	13.57	10.81	0.8422	0.986	0.9993	0.9998	0.9999	0.9896	0.9912	0.6469	0.8944	0.9974	0.998
	<i>R</i> ²	0.8422	0.986	0.9993	0.9998	0.9999	0.9999	0.9896	0.9912	0.6469	0.8944	0.9974	0.998	0.9999	0.9999	0.9999	0.9999	0.9999	0.9999	0.9999	0.9999	0.9999	0.9999	0.9999
CO	<i>SSE</i>	23.25	0.641	0.1548	0.04609	0.1183	0.05244	2.011	0.388	35.4	17.79	0.1917	0.09578	0.5965	0.9889	0.9973	0.9979	0.9991	0.9651	0.9933	0.3856	0.6912	0.9967	0.9983
	<i>R</i> ²	0.5965	0.9889	0.9973	0.9989	0.9979	0.9991	0.9651	0.9933	0.3856	0.6912	0.9967	0.9983	0.9999	0.9999	0.9999	0.9999	0.9999	0.9999	0.9999	0.9999	0.9999	0.9999	0.9999
NO	<i>SSE</i>	7.23	0.1791	0.04549	0.02719	0.02662	0.009658	1.35	0.2585	12.33	6.111	0.04954	0.03855	0.7146	0.9929	0.9982	0.9989	0.9994	0.9467	0.9898	0.5134	0.7588	0.998	0.9985
	<i>R</i> ²	0.7146	0.9929	0.9982	0.9989	0.9989	0.9994	0.9467	0.9898	0.5134	0.7588	0.998	0.9985	0.9999	0.9999	0.9999	0.9999	0.9999	0.9999	0.9999	0.9999	0.9999	0.9999	0.9999

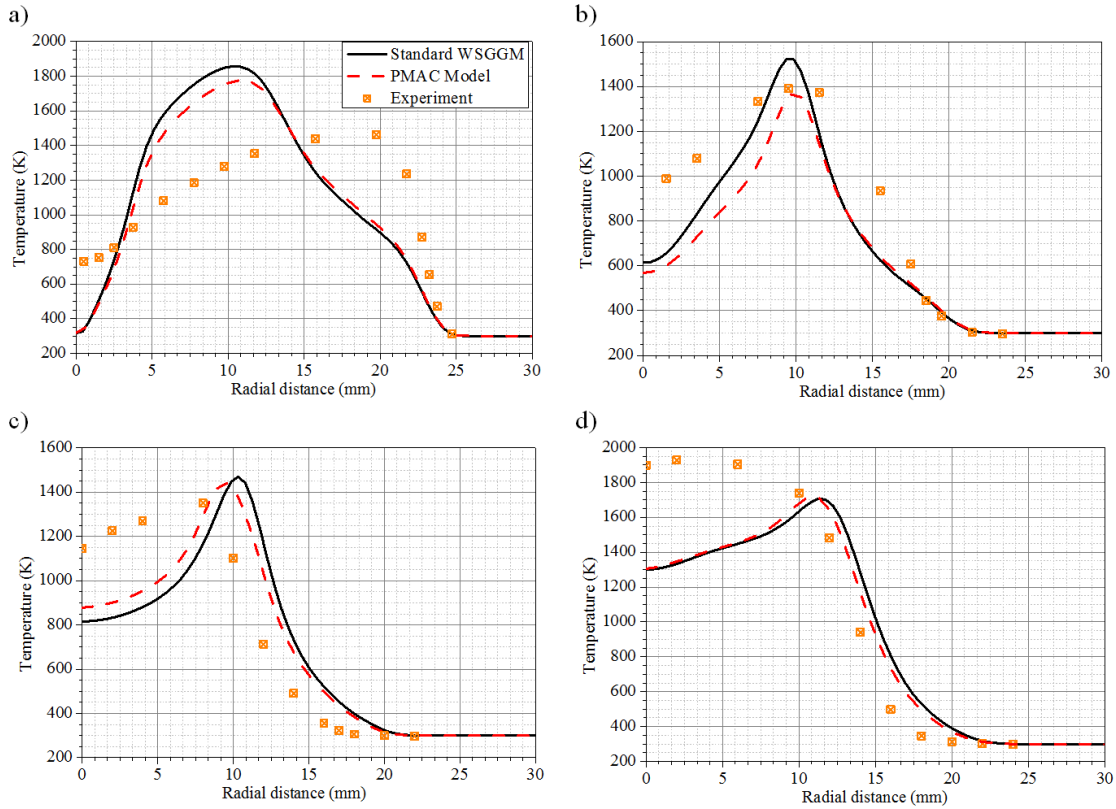


Figure 5: Temperature profiles at several downstream locations. a) $x = 20$ mm, b) $x = 40$ mm, c) $x = 55$ mm, d) $x = 75$ mm

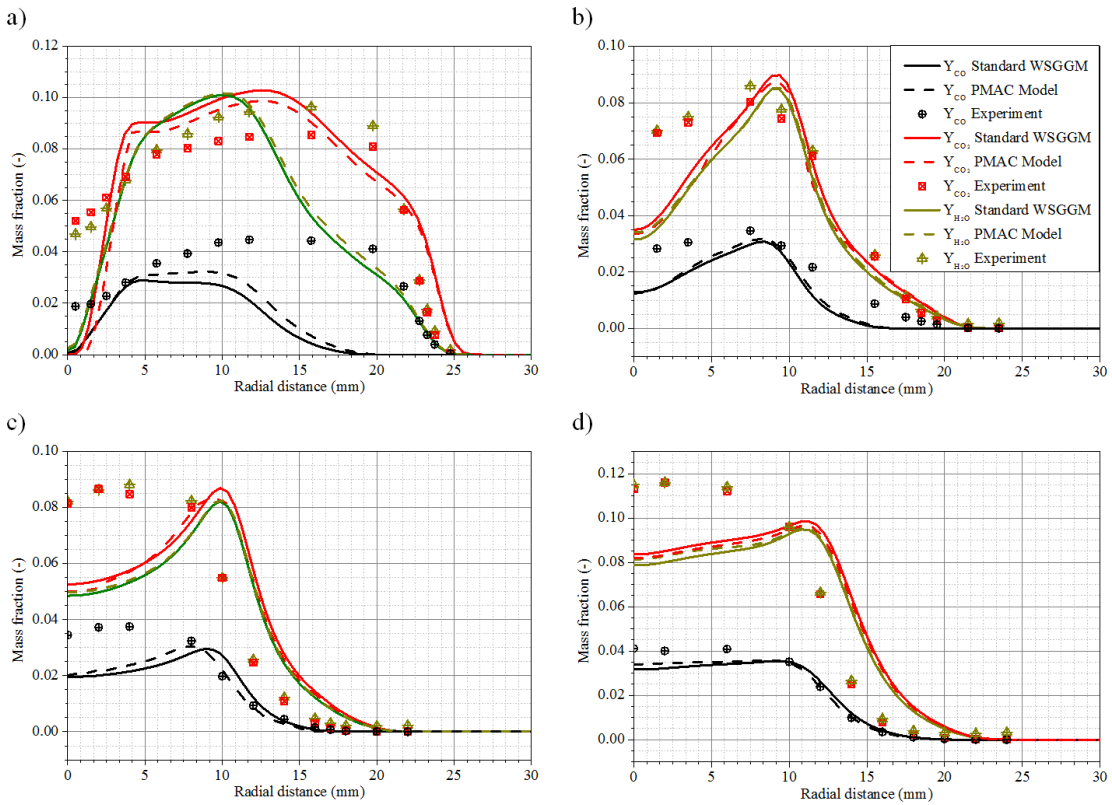


Figure 6: CO, CO₂ and H₂O Mass fraction profiles at several downstream locations. a) $x = 20$ mm, b) $x = 40$ mm, c) $x = 55$ mm, d) $x = 75$ mm

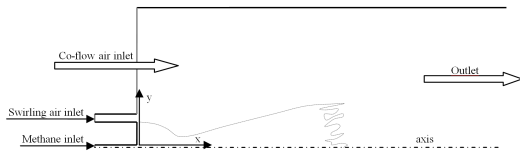


Figure 3: Swirling Turbulent Non-premixed Flames of Methane experiment

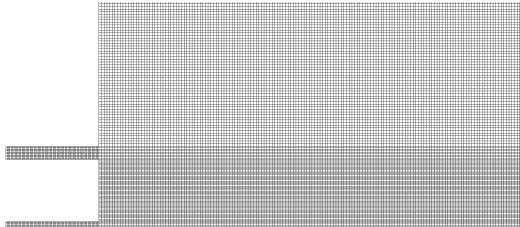


Figure 4: Computational grid for numerical calculations in the methane and swirling air inlets region (inlet area).

modeled with a realizable $k - \varepsilon$ model and standard wall function. Walls were treated as adiabatic.

A mesh convergence test with the use of an adaptation tool in ICEM CFD was performed. Solutions were obtained for four grids of the following number of cells: 68163, 85152, 135635, 170901. The discrepancy in peak temperature measured 20 mm above the co-flow air inlet were equal: 5.21%, 1.92%, 0.97%. Since the discrepancy between the results obtained with the use of the last two grids was lower than 1%, the last grid is used in further calculations.

Uniform velocity profiles at each inlet were assumed. This is an appropriate assumption since the swirling air and methane inlet diameters used in the experimental burner are a couple of times smaller than their lengths, thus providing an appropriate distance to unify the flow. Moreover, the grid for inlets was extended in order to capture the impact of the fully developed boundary layer (Fig. 4). The turbulence intensity of co-flow air is assumed to be 2% according to experimental data.

Boundary conditions at 20 mm radial distance above the air co-flow inlet were verified against experimental data [12]. The maximum calculated discrepancy of radial and swirl velocity in relation to the experiment was 4.3%. Based on this, the assumed boundary conditions are in good agreement with the experimental data.

In Fig. 5, a comparison between standard WSGGM, PMAC Model and experimental data is shown. The results are analyzed on four selected planes located at $x = 20$ mm, 40 mm, 55 mm and 77 mm. Based on this comparison it can be observed that, in each location, the peak temperature calculated using proposed model is closer to

the experimental data. Peak temperature calculated using the PMAC Model is lower for every location. The maximum calculated relative discrepancy of the peak temperature among models is up to 14% at $x = 40$ mm. At the same location one may also observe the best agreement of results obtained from the PMAC approach with the experimental data. The reason why the proposed PMAC model results adapt better to the experimental data is the direct link between the absorption coefficient and the mole fraction of individual species in the reagents mixture. Inclusion of absorption coefficient of two additional species has also significant effect on results improvement towards experimental data. Standard WSGGM overestimates flame temperatures, therefore it may have a significantly impact on NO_x predictions. The presented temperature profiles show that radiative heat transfer has a large influence on the results when used with an equilibrium chemistry non-premixed combustion. It is suspected that incorporating larger quantities of species and utilization of a more complex chemistry model (such as GRI-Mech 3.0) during the numerical calculation can improve results towards the experimental data.

Fig. 6 shows profiles of Reynolds averaged mass fractions of CO, CO₂ and H₂O from experiment and numerical calculations for both: standard WSGGM and PMAC models. Significant improvements observed for CO mass fraction profiles (up to 22% at $x = 20$ mm). CO₂ mass fraction profiles show up to 6% improvement towards experimental data at $x = 20$ mm. Mass fraction profiles of H₂O obtained by both models are the closest to each other from all of the considered species (maximum discrepancy up to 14% at $x = 40$ mm) for all of the downstream locations. All of the profiles presented for PMAC Model are closer to the experimental data than those obtained with the use of standard WSGGM.

The discrepancy between the results of numerical calculations for the standard WSGGM and PMAC model against the experimental data is partially caused by the fuel mixture used in the experiment. Numerical calculations presented in this paper adopted air as a mixture of the 79% mole fraction of nitrogen and 21% of oxygen. As regards the fuel, pure methane was assumed in the calculations. Significant variation occurs in the experiment, but the presented experimental results are only Reynolds averaged mass fractions. To give an example of an experimental data variation, the standard deviation of peak combustion temperature at the location $x=20$ mm is equal to 42% of the mean value. This shows how unstabilized combustion processes are and how hard they are to simulate with RANS equations. It is extremely difficult to recre-

ate conditions during the experiment in numerical calculations and usually it can be done only to a certain degree of an approximation. The adopted PMAC Model determines the absorption coefficients of non-modeled reagents as equal to zero, which in general introduces errors (especially in relation to a CH_4 which is not included in HITEMP 2010). Finally, as mentioned in the introduction, the developed model is planned to be used in order to obtain only approximate, initial solutions. Final calculations are to be performed with the use of more complex reaction mechanisms.

5. Conclusions

The proposed approach to an H_2O , CO_2 , CO and NO Planck Mean Absorption Coefficients Model for radiation numerical modelling in combustions flows has been developed and successfully implemented into the ANSYS FLUENT commercial CFD code. The approach was verified with the use of turbulent non-premixed methane combustion with swirling air experimental data. The proposed PMAC Model shows slightly better results (closer to the experimental data) than the currently available standard WSGGM used with the equilibrium chemistry non-premixed combustion model. The strengths of the proposed model can be noticed in rapid (coarse) combustion calculations in which significant benefits are observed alongside insignificant increase in calculation time.

The proposed Planck Mean Absorption Coefficients Model for radiation numerical modeling in combustion simulations can be used in a wide range of numerical codes and adjusted to individual needs. It can be extended to any number of combustion species and any reaction mechanism.

References

- [1] C. E. Baukal, Heat Transfer in Industrial Combustion, CRC Press, 2000.
- [2] A. Lefebvre, Gas Turbine Combustion, Taylor & Francis, 1999.
- [3] A. Schultz, Convective and radiative heat transfer in combustors, Tech. rep., Institute für Thermische Stromungsmaschinen, Universität Karlsruhe (1999).
- [4] H. L. S. Matarazzo, Modelling of the heat transfer in a gas turbine liner combustor (September 2011).
- [5] V. Arpaci, R. Tabaczynski, Radiation-affected laminar flame propagation, Combustion and flame 46 (1982) 315–322.
- [6] J. M. C. H. H. Brocklehurst, Scot and Radiation Modeling in Gas Turbine Combustion Chambers, Rolls-Royce plc, 1999.
- [7] R. Cookson, An investigation of heat transfer from flames, Ph.D. thesis, University of Leeds (1960).
- [8] R. Barlow, A. Karpetis, J. H. Frank, J.-Y. Chen, Scalar profiles and no formation in laminar opposed-flow partially premixed methane/air flames, Combustion and Flame 127 (2001) 2102–2118.
- [9] W. Grosshandler, RADCAL: A Narrow-Band Model for Radiation Calculations in a Combustion Environment, Tech. Rep. 1402, NIST (1993).
- [10] X. L. Zhu, J. P. Gore, A. N. Karpetis, R. S. Barlow, The effects of self-absorption of radiation on an opposed flow partially premixed flame, Combustion and Flame 129 (2002) 342–345.
- [11] L. Rothman, I. G. R.J., B. H. Dothe, R. Gamache, A. Goldman, V. Perevalov, S. Tashkun, J. Tennyson, HITEMP, the high-temperature molecular spectroscopic database, Journal of Quantitative Spectroscopy & Radiative Transfer 111 (2010) 2139–2150.
- [12] P. Kalt, Y. Al-Abdeli, A. Masri, R. Barlow, Swirling turbulent non-premixed flames of methane: Flowfield and compositional structure, Proc. Combust. Inst. 29 (2002) 1913–1919.
- [13] Y. Al-Abdeli, A. Masri, Recirculation and flow field regimes of unconfined non-reacting swirling flows, Experimental Thermal and Fluid Sciences 27 (2003) 655–665.
- [14] Y. Al-Abdeli, A. Masri, Stability characteristics and flow fields of turbulent swirling jet flows, Combust. Theory and Modeling 7 (2003) 731–766.
- [15] A. Masri, P. Kalt, R. Barlow, The compositional structure of swirl-stabilised turbulent non-premixed flames, Combustion and Flame 137 (2004) 1–37.
- [16] Y. Al-Abdeli, A. Masri, Precession and recirculation in turbulent swirling isothermal jets, Combust. Sci. Technol. 176 (2004) 645–665.
- [17] A. Inc., ANSYS FLUENT 14 Theory Guide (November 2011).
- [18] T. F. Smith, Z. F. Shen, J. N. Friedman, Evaluation of coefficients for the weighted sum of gray gases model, J. Heat Transfer. 104 (1982) 602–608.
- [19] A. Coppalle, P. Vervisch, The total emissivities of high-temperature flames, Combustion and Flame 49 (1983) 101–108.
- [20] C. L. Tien, W. H. Giedt, Experimental determination of infrared absorption of high-temperature gases in advances in thermophysical properties at extreme temperatures and pressures, ASME 49.
- [21] The MathWorks Inc., MATLAB: Data Analysis (September 2013).
- [22] Radiation Models, <http://www.sandia.gov/tnf/radiation.html> ([Online; accessed September 23, 2014]).
- [23] A. Inc., ANSYS FLUENT 14: ANSYS Fluid Dynamics Verification Manual (August 2011).